Investigation of Collisions between Li($2P$) Atoms and Electrons: Excitation of $4l$ Levels

A. Pietruczuk and T. Stacewicz*

Institute of Experimental Physics, Warsaw University
Hoża 69, 00-681 Warsaw, Poland

(Received January 8, 2003; in final form March 6, 2003)

Results of measurements of rate constants for transitions between $2P \rightarrow 4S$, $2P \rightarrow 4P$, and $2P \rightarrow 4D$ levels of lithium are presented. The investigations were performed in laser induced plasma. The results were compared with calculations based on Born and close coupling approach.

PACS numbers: 34.80.–i, 34.80.Dp

1. Introduction

Collisions of electrons with atoms have been investigated since more than one hundred years. In spite of that only few experimental studies have been done with the excited atoms (excluding the atoms in metastable levels). This is caused by the huge technical problems. Therefore data for these kind of impacts are available primarily from theoretical papers. These data are of great importance for plasma physics, astrophysics, physics of the new light sources, etc. For alkali atoms, besides the classical calculations [1, 2], the quantum approaches based on Born approximation [3] and close coupling approximation [4] are known. Unfortunately, results of these calculations differ significantly. It concerns especially the range of very low electron energy which corresponds to a low temperature plasma.

The experiments were done mainly with Na($3P$) sodium atoms [5, 6], however, majority of them concerns the superelastic scattering of electrons leading to $3P$–$3S$ transition [7–17]. The investigations of e–Li($2P$) superelastic collisions were reported as well [18].

*corresponding author; e-mail: tadstac@fuw.edu.pl

In our recent paper [19] we presented the rate constants for e–Li($2P$) collisions leading to excitation of $3S$, $3P$, and $3D$ levels. Here we show results of measurement of the rate constants for electron impact induced transitions between $2P$ and $4l$ levels of lithium.

2. Experiment

Details of the experiment were shown in our previous papers [16, 17, 19], therefore here only a brief description is presented. The measurements were performed in a heat-pipe oven at a temperature of 400°C which contained a mixture of lithium and sodium with 10 Torr of argon as a buffer gas. Concentration of sodium vapor which served as the electron generator was about 10^{15} cm^{-3}. Concentration of lithium vapor was about three orders of magnitude lower.†

The experimental setup is presented in Fig. 1. The measurements were done in plasma produced by light pulse from the LASER589 tuned to the resonance transition (589 nm). Here the collisional process of the plasma production in sodium was used [22]. It provides the electrons of the density about 10^{11} cm^{-3} and the temperature of several thousand kelvins. The energy of the pulse was about 2–3 mJ, its FWHM time — about 7 ns and the spectral line width — about 0.01 nm. The electrode placed in the cell served as the Langmuir plasma probe and was used to determine the electron temperature and for evaluation of the electron density. The probe current was analyzed by means of a digital oscilloscope. In order to reduce

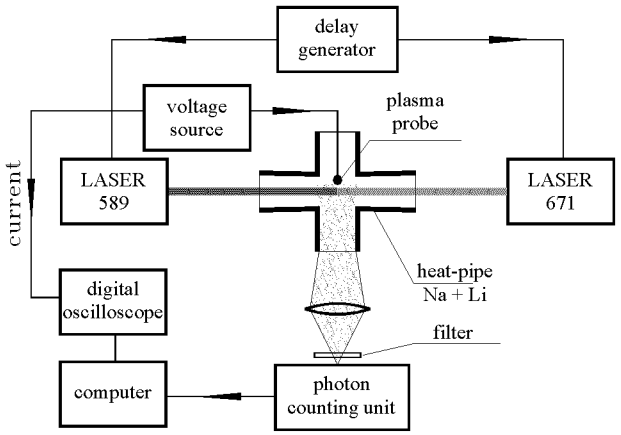

Fig. 1. The experimental setup.

†Number densities given by Nesmeyanov [20] (6×10^{15} cm^{-3} for Na and 1.4×10^{12} cm^{-3} for Li at 400°C) concern the saturated vapors. Usually this condition is not fulfilled in heat pipes where the concentrations even one order of magnitude lower were observed [21].

uncertainties of the electron temperature caused by a high pressure of the buffer gas (affecting the Langmuir plasma probe measurements) a specially developed method of elaboration of the plasma probe data was applied [22].

The second dye laser (LASER671) tuned to the resonance transition in lithium (671 nm) was used for production of the Li($2P$) atoms. The energy of the pulses from this laser was about 0.5 mJ, their FWHM time — about 7 ns. The light beam producing the Li($2P$) atoms was introduced into the cell collinearly with the ionizing beam. The diameter of both laser beams in the cell was equal to $2a = 8$ mm.

Both lasers were synchronized by a delay generator. The frequency of repetition of the light pulses was equal to 7 Hz. At each trigger pulse the process of measurements was initiated by the shot of the dye LASER589 producing the plasma. Within several microseconds the temperature and the concentration of electrons were well stabilized. Then with a delay of 6 μs the pulse from the LASER671 was generated. Due to collisions of the electrons with Li($2P$) atoms the higher lying levels (among them $4l$) were populated. By measuring a fluorescence signal at lines originating from these levels the rate constants for the electron impact induced transitions $2P \rightarrow 4l$ were determined. The respective wavelengths of the observed fluorescence (497, 460, and 274 nm — see Fig. 2) were selected by means of a monochromator and a set of color and interference filters. The photomultiplier connected to the digital oscilloscope controlled by means of a special software served as the photon counting system [23].

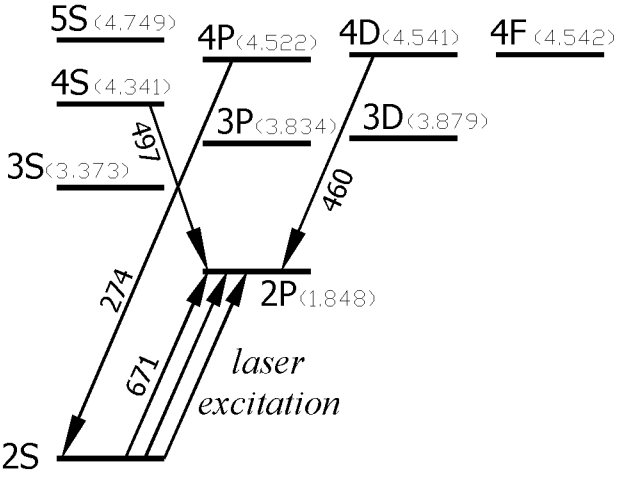

Fig. 2. Scheme of transitions observed in the experiment in case of lithium. In brackets energies of the levels [eV] are given.

3. Analysis of the experiment

The evolution of Li($4l$) atoms distribution, $N_{4l}(\boldsymbol{r},t)$, is given by the differential equation

$$\frac{\mathrm{d}N_{4l}(\boldsymbol{r},t)}{\mathrm{d}t} = -A_{4l}N_{4l}(\boldsymbol{r},t) + k_{2P\to 4l}(T_\mathrm{e})N_\mathrm{e}(\boldsymbol{r},t)N_{2P}(\boldsymbol{r},t). \tag{1}$$

The terms at the right side describe the spontaneous emission with the Einstein coefficient, A_{4l}, and the population of the $4l$ level due to electron impact excitation from the $2P$ level. Here $k_{2P\to 4l}(T_\mathrm{e})$ denotes the collisional rate constant for the respective transition at given electron temperature T_e, $N_\mathrm{e}(\boldsymbol{r},t)$ — the electron distribution and $N_{2P}(\boldsymbol{r},t)$ — distribution of Li($2P$) atoms excited by the laser pulse. We neglect the radiative and collisionally induced transitions populating the $4l$ level from the states other than that one excited by the laser as well as collisions depopulating the $4l$ level.‡

Solution of Eq. (1) provides opportunity to describe the experimental signal: number of the fluorescence photons registered by the detector on respective wavelength. However, in order to find the $N_\mathrm{e}(\boldsymbol{r},t)$ function the analysis of the plasma diffusion must be performed, while the determination of $N_{2P}(\boldsymbol{r},t)$ distribution requires the analysis of the resonance radiation trapping.

We can assume that in the heat pipe the cylindrical geometry is fulfilled. Therefore diffusion of the electrons is described by the following equation:

$$\frac{\partial N_\mathrm{e}(r,t)}{\partial t} = D_\mathrm{A}\frac{1}{r}\frac{\partial}{\partial r}\left[r\frac{\partial}{\partial r}N_\mathrm{e}(\boldsymbol{r},t)\right], \tag{2}$$

where D_A denotes the ambipolar diffusion coefficient which is related to the decay time τ of the main mode of plasma diffusion: $D_\mathrm{A} = a^2/\tau p_1^2$ ($p_1 = 2.404$ is the root of the Bessel function of zero order and the first kind [24], a is the radius of heat pipe). In our experiment value of the τ parameter reached about 100 μs. It was measured by registration of the ionic current with the plasma probe [25]. Since the process of the electron production takes place only within several tens of nanosecond after the LASER589 shot [26] we assume that the electrons are generated mainly in the region determined by the laser beam. The diffusion Eq. (2) provides opportunity to find the $N_\mathrm{e}(\boldsymbol{r},t)$ function.

The $N_{2P}(\boldsymbol{r},t)$ function can be found by analysis of the resonance light diffusion. Spectral line width of LASER671 (about 0.05 nm) is large enough to overlap both fine-structure components of resonance line in lithium (670.791 and 670.776 nm). Therefore Li($2P$) population should be described by sum of population of each sublevel: $N_{2P}(\boldsymbol{r},t) = N_{2P1/2}(\boldsymbol{r},t) + N_{2P3/2}(\boldsymbol{r},t)$ and the integro-differential equation of the light diffusion [27]:

$$\frac{\partial N_{2PJ}(\boldsymbol{r},t)}{\partial t} = -A_{2P}N_{2PJ}(\boldsymbol{r},t) + A_{2P}\int_V N_{2PJ}(\boldsymbol{r}',t)G_J(\boldsymbol{r},\boldsymbol{r}')d^3\boldsymbol{r}' \tag{3}$$

‡This assumption is based on analysis of respective rate constants which were evaluated using the theoretically calculated cross-sections [4].

must be solved for each fine-structure component ($J = 1/2, 3/2$). The integration is done over whole volume of the cell, V. Here A_{2P} denotes the rate of spontaneous decay of Li($2P$) atoms. $G_J(\boldsymbol{r}, \boldsymbol{r}')$ is the probability that the resonance photon emitted in any point $\boldsymbol{r}'$ is reabsorbed in the point of interest $\boldsymbol{r}$:

$$G_J(\boldsymbol{r}, \boldsymbol{r}') = \frac{1}{4\pi|\boldsymbol{r} - \boldsymbol{r}'|^2} \int_0^\infty \mathrm{d}\nu P_J(\nu) k_J(\nu) \exp[-|\boldsymbol{r} - \boldsymbol{r}'| k_J(\nu)], \tag{4}$$

where $P_J(\nu)$ is a normalized shape of the emission line for a given fine-structure component, while $k_J(\nu)$ is the relevant absorption coefficient. Since under conditions of our experiment the Doppler broadening dominates, both coefficients are described by the Gaussian functions[§]

$$P(\nu_J) = \frac{c}{\sqrt{\pi}\nu_J V_0} \exp\left[-\frac{(\nu - \nu_J)^2}{\nu_J^2} \frac{c^2}{V_0^2}\right],$$

$$k_J(\nu) = k_0^J \exp\left[-\frac{(\nu - \nu_J)^2}{\nu_J^2} \frac{c^2}{V_0^2}\right]. \tag{5}$$

Here ν_J denotes the frequency of transition, c is the light speed, $V_0 = \sqrt{\frac{2kT_\mathrm{C}}{M}}$ — mean velocity of atoms at the gas temperature T_C, k — the Botzmann constant and M — the atomic mass. According to Holstein [27], for cylindrical geometry the absorption coefficient k_0^J at the center of the line can be found from the equation

$$k_0^J a = \frac{1.6\tau_1^J A_{2P}}{\sqrt{\pi \ln(k_0^J a)}}, \tag{6}$$

where τ_1^J denotes time of the radiation imprisonment. This time was measured during the experiment.

The knowledge of $N_{2P}(\boldsymbol{r}, t)$ and $N_\mathrm{e}(\boldsymbol{r}, t)$ functions provides opportunity to find the function $N_{4l}(\boldsymbol{r}, t)$ describing concentrations of highly excited levels. Solving Eq. (1) one obtains

$$N_{4l}(\boldsymbol{r}, t) = k_{2P\to 4l}(T_\mathrm{e}) \exp(-A_{4l}t) e(\boldsymbol{r}) \int_{t2}^t \mathrm{d}t' N_\mathrm{e}(\boldsymbol{r}, t) N_{2P}(\boldsymbol{r}, t') \exp(A_{4l}t'). \tag{7}$$

The integration starts at the moment $t2$ of the LASER671 pulse. The number of fluorescence photons that were emitted by the Li($4l$) atoms and were registered per unit of time by the detector localized in $\boldsymbol{R}'$ is equal to

$$n_{4l}^F(t) = \Phi_{4l} A_{4l\to n'l'} \Delta S \int_V \frac{\mathrm{d}^3 r}{4\pi|\boldsymbol{R}' - \boldsymbol{r}|^2} N_{4l}(\boldsymbol{r}, t), \tag{8}$$

where Φ_{4l} denotes quantum efficiency of the optical system for the respective wavelength and $A_{4l\to n'l'}$ — the respective rate constant for spontaneous emission of registered transition, ΔS — the surface of the detector. The integration is done

[§]The hyperfine splitting of lithium resonance lines are small enough for approximating the absorption line profile by the Gaussian function with the width of about 5% larger than the Doppler width of a single frequency line.

over whole volume of the cell V. During the experiment the number of photons was integrated over the time period $T = 2$ μs. Then number of the registered counts is expressed by

$$N_{4l}^F = \int_{t2}^{t2+T} \mathrm{d}t n_{4l}^F(t) = \Phi_{4l} A_{4l\to n'l'} \Delta S \int_{t2}^{t2+T} \mathrm{d}t \int_V \mathrm{d}^3 r \frac{N_{4l}(\boldsymbol{r},t)}{4\pi|\boldsymbol{R}'-\boldsymbol{r}|^2}$$
$$= \Phi_{4l} A_{4l\to n'l'} \Delta S k_{2P\to 4l}(T_\mathrm{e}) \int_{t2}^{t2+T} \mathrm{d}t \int_V \frac{\mathrm{d}^3 r e(\boldsymbol{r})}{4\pi|\boldsymbol{R}'-\boldsymbol{r}|^2} \exp(-A_{4l}t)$$
$$\times \int_{t2}^{t} \mathrm{d}t' N_\mathrm{e}(\boldsymbol{r},t') N_{2P}(\boldsymbol{r},t') \exp(A_{4l}t'). \tag{9}$$

Replacing the triple integral in the above equation by symbol X one gets

$$N_{4l}^F = \Phi_{4l} A_{4l\to n'l'} \Delta S k_{2P\to 4l}(T_\mathrm{e}) X. \tag{10}$$

Determination of the rate constant $k_{2P\to 4l}(T_\mathrm{e})$ from Eq. (9) is difficult since the parameters like the absolute values of concentration of the laser excited atoms $N_{2P}(\boldsymbol{r},t)$ and electrons $N_\mathrm{e}(\boldsymbol{r},t)$ are hard to measure and they are usually affected by a large experimental error. In order to avoid this difficulty we used a reference signal. For this purpose the resonance fluorescence at the transition 671 nm was applied. The reference signal was registered when the cell was irradiated by pulses from the LASER589 only. In this case the resonance fluorescence from Li($2P$) atoms is excited due to collisions of Li($2S$) atoms with the electrons. For each fine-structure sublevel evolution of concentration of the resonantly excited atoms is described by the equation of the light diffusion with excitation [27]:

$$\frac{\mathrm{d}N_{2PJ}^R(\boldsymbol{r},t)}{\mathrm{d}t} = -A_{2P} N_{2PJ}^R(\boldsymbol{r},t) + k_{2S\to 2P}(T_\mathrm{e}) N N_\mathrm{e}(\boldsymbol{r},t)$$
$$+ A_{2P} \int_V \mathrm{d}^3 r' N_{2PJ}^R(\boldsymbol{r}',t) G_{2P}^J(\boldsymbol{r},\boldsymbol{r}'). \tag{11}$$

Number of photons registered per time unit at resonance line is equal to

$$n_J^R(t) = \Phi_\mathrm{R} A_i \Delta S \int_V \frac{\mathrm{d}^3\mathrm{r}}{4\pi|\boldsymbol{R}'-\boldsymbol{r}|^2} N_{2PJ}^R(\boldsymbol{r},t) T_J(\boldsymbol{R}',\boldsymbol{r}) = \Phi_\mathrm{R} A_{2P} k_{2S\to 2P}(T_\mathrm{e})$$
$$\times \Delta S \int_V \frac{\mathrm{d}^3\mathrm{r}}{4\pi|\boldsymbol{R}'-\boldsymbol{r}|^2} N_\mathrm{e}(\boldsymbol{r},t) N_{2PJ}^R(\boldsymbol{r},t) T_J(\boldsymbol{R}',\boldsymbol{r}), \tag{12}$$

where Φ_R denotes the quantum efficiency of the optical system at the resonanceline. Since the resonance radiation is strongly absorbed by the vapor we consider also its transmission coefficient $T_J(\boldsymbol{R}',r)$ that is equal to

$$T_J(\boldsymbol{R}',r) = \int_0^\infty \mathrm{d}\nu P(\nu_J) \exp[-|\boldsymbol{R}'-\boldsymbol{r}| k_J(\nu_J)], \tag{13}$$

where $\boldsymbol{R}'$ denotes the position of the light detector. We neglect the excitations due to secondary collisions as well as the cascade transitions from higher excited levels. Finally the total reference signal registered at both fine-structure components integrated over the time T per one laser pulse is expressed by

$$N^R = \Phi_{\mathrm{R}} A_{2P} k_{2S\to 2P}(T_{\mathrm{e}}) \Delta S \int_{t2}^{t2+T} \mathrm{d}t \int_V \frac{N_{\mathrm{e}}(r)\mathrm{d}^3 r}{4\pi |\boldsymbol{R}' - \boldsymbol{r}|^2}$$

$$\times [N^R_{2P1/2}(\boldsymbol{r},t) T_{1/2}(\boldsymbol{R}',\boldsymbol{r}) + N^R_{2P3/2}(\boldsymbol{r},t) T_{3/2}(\boldsymbol{R}',\boldsymbol{r})]. \tag{14}$$

Replacing the double integral in the above equation by symbol Y, one gets

$$N^R = \Phi_{\mathrm{R}} A_{2P} k_{2P\to 2S}(T_{\mathrm{e}}) Y. \tag{15}$$

Combining Eqs. (10) and (15) the ratio of the rate constant can be expressed by

$$\frac{k_{2P\to 4l}(T_{\mathrm{e}})}{k_{2S\to 2P}(T_{\mathrm{e}})} = \frac{N_{4l}}{N^R} \frac{\Phi_{\mathrm{R}}}{\Phi_{4l}} \frac{A_{2P}}{A_{4l\to n'l'}} \frac{X}{Y}. \tag{16}$$

Here except the atomic constants A_{2P} and $A_{4l\to n'l'}$ [28] the other quantities, i.e.: Φ_{R}, Φ_{4l}, N_{4l}, and N^R were determined in the experiment. The X and Y integrals were calculated numerically. Since both X and Y depend linearly on the atomic and electronic concentration, one can avoid the doubtful determination of these parameters. The cross-section $\sigma_{2S\to 2P}(E)$ for electron impact excitation of the resonance transition in lithium was measured by many authors [29–31]. This cross-section can be used for calculation of the $k_{2S\to 2P}(T_{\mathrm{e}})$ constant

$$k_{2S\to 2P}(T_{\mathrm{e}}) = \int_0^\infty \sigma_{2S\to 2P}(E) f(E,T_{\mathrm{e}}) \sqrt{\frac{2E}{m_{\mathrm{e}}}} \mathrm{d}E, \tag{17}$$

where $f(E,T_{\mathrm{e}})$ denotes Maxwellian distribution of the electron energy E, m_{e} — electron mass.

4. Discussion and results

In our consideration we neglected the collisions mixing the population between Li($4l$) levels. As is seen in Fig. 2 the energy gap between $4P$, $4D$, and $4F$ level is smaller than kT_{C}. Dubreil and Chaleard [32] showed that at the argon pressure higher than 8 Torr, due to inelastic collisions of Li($4P$), Li($4D$), and Li($4F$) atoms with Ar atoms, the populations of these levels become completely mixed within a nanosecond time scale. Population mixing by argon is also supported by the electron impact induced transitions between these levels. Using the cross-sections by Schweinzer et al. [4] we found that for the electron temperatures observed in our experiment ($T_{\mathrm{e}} = 4000 \div 10000$ K) the rates for the population exchange can be higher than 10^{-4} cm^3 s^{-1}, so at the electron concentrations of 10^{11} cm^{-3} the efficiency of the electronic mixing is comparable with the mixing due to collisions with argon. Therefore $4P$, D, F levels behave as a single level which relax with the same rate. For this reason Eq. (1) should be modified as follows:

$$\frac{\mathrm{d}N^{\mathrm{eff}}_{4PDF}(\boldsymbol{r},t)}{\mathrm{d}t} = -A^{\mathrm{eff}}_{4PDF} N^{\mathrm{eff}}_{4PDF}(\boldsymbol{r},t) + k^{\mathrm{eff}}_{2P\to 4PDF}(T_{\mathrm{e}}) N_{\mathrm{e}}(\boldsymbol{r},t) N_{2P}(r,t), \tag{18}$$

where $N^{\mathrm{eff}}_{4PDF} = N_{4P} + N_{4D} + N_{4F}$. The effective decay rate of the mixed levels

$$A^{\text{eff}}_{4PDF} = \frac{g_{4P}A_{4P} + g_{4D}A_{4D} + g_{4F}A_{4F}}{g_{4P} + g_{4D} + g_{4F}}, \tag{19}$$

where g_{4l} denote statistic weights of the respective levels. In this case the effective rate of the $2P \rightarrow 4P, D, F$ levels population due to the electron impact is defined as follows:

$$k^{\text{eff}}_{2P\rightarrow 4PDF}(T_{\text{e}}) = k_{2P\rightarrow 4P}(T_{\text{e}}) + k_{2P\rightarrow 4D}(T_{\text{e}}) + k_{2P\rightarrow 4F}(T_{\text{e}}). \tag{20}$$

The population of each $4P$, $4D$, and $4F$ level as well as their rates of spontaneous decay follows from the statistical ratio:

$$N_{4l} = \frac{g_{4l}}{g_{4P} + g_{4D} + g_{4F}} N^{\text{eff}}_{4PDF} \tag{21a}$$

and

$$A^{\text{eff}}_{4PDF\rightarrow n'l'} = \frac{g_{4l}}{g_{4P} + g_{4D} + g_{4F}} A_{4l\rightarrow n'l'}. \tag{21b}$$

Therefore in Eqs. (7), (9), (10), and (16) the effective parameters expressed by the formulae (20), (21) should be used. The population mixing is the reason that in our experiment only the effective rate constant $k^{\text{eff}}_{2P\rightarrow 4PDF}(T_{\text{e}})$ can be determined.

The results of measurement of this rate are shown in Fig. 3. The experimental data represented by points are compared with calculations based on close coupling approximations [4].¶ Uncertainty of the electron temperature measurements is about ±10%. The error of the determination of the $k_{2P\rightarrow 4PDF}(T_{\text{e}})/k_{2S\rightarrow 2P}(T_{\text{e}})$ reaches 50%.

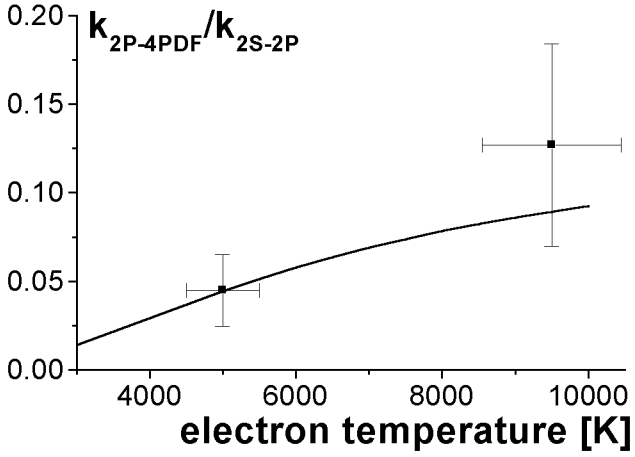

Fig. 3. Effective rate constants for electron impact induced transition between $2P \rightarrow 4P, D, F$ levels. Cw lines represent the rates calculated using the cross-section by Schweinzer et al. [4].

¶These results cannot be compared with calculations by Krishnan and Stumpf [3] since they do not provide the cross-section for $2P \rightarrow 4P$ and $2P \rightarrow 4F$ transitions.

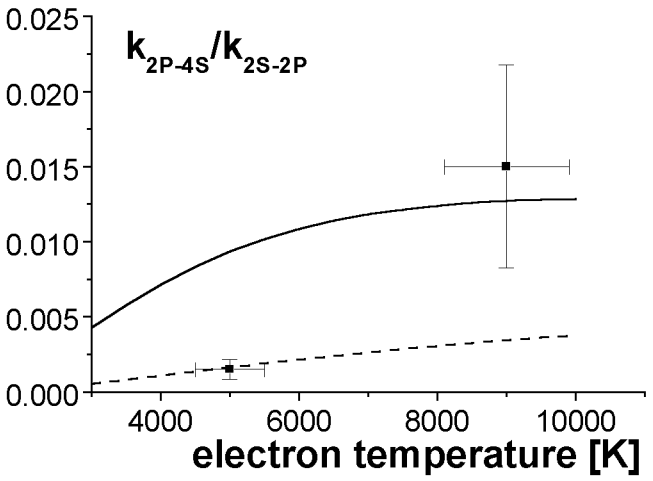

Fig. 4. Rate constants for $2P \rightarrow 4S$ transition compared with theoretical calculations: cw lines — close coupling approximation [4], dashed line — Born approximation [3].

The population mixing can be neglected in the case of the $4S$ level. Here the energy gaps with respect to the neighbor levels ($4P$, $3D$) are about one order of magnitude larger than that between $4P, D, F$ levels (see Fig. 2) and the rate constants for the population mixing due to collisions with the electrons are about two orders of magnitude lower. Also collisions with argon do not change the population of Li($4S$) level significantly [33]. Results of measurements of $k_{2P\rightarrow 4S}(T_e)/k_{2S\rightarrow 2P}(T_e)$ ratio was shown in Fig. 4. At low electron temperature (5000 K) the experimental data agree better with the rates calculated with the Born approximation [3] while at 9500 K our result corresponds to the close coupling approach.

Acknowledgments

This work was supported by the State Committee for Scientific Research, grant number 2 P03B 050 18.

References

[1] M. Gryziński, *Phys. Rev.* **138,** A305 (1965).

[2] M. Gryziński, *Phys. Rev.* **138,** A336 (1965).

[3] U. Krishnan, B. Stumpf, *At. Data Nucl. Data Tables* **51,** 151 (1992).

[4] J. Schweinzer, R. Brandenburg, I. Bray, R. Hoekstra, F. Aumayr, R.K. Janev, H.P. Winter, *At. Data Nucl. Data Tables* **72,** 239 (1999).

[5] B. Stumpf, A. Gallagher, *Phys. Rev. A* **32,** 3344 (1985).

[6] T.T. Jiang, M. Zuo, L. Vušković, B. Bederson, *Phys. Rev. Lett.* **68,** 915 (1992).

[7] I.V. Hertel, W. Stoll, *J. Phys. B* **7,** 583 (1974).

[8] H.W. Hermann, I.V. Hertel, W. Reiland, A. Stamatovic, W. Stoll, *J. Phys. B* **10,** 251 (1977).

[9] H.W. Hermann, I.V. Hertel, *Z. Phys. A* **307,** 89 (1982).

[10] D.F. Register, S. Trajmar, G.C. Csanak, W. Jensen, M.A. Fineman, R.T. Poe, *Phys. Rev. A* **28,** 151 (1983).

[11] G.F. Hanne, Cz. Szmytkowski, M.J. Van der Wiel, *Phys. B* **15,** L109 (1982).

[12] J.J. McClelland, M.H. Kelley, R.J. Celotta, *Phys. Rev. A* **40,** 2321 (1989).

[13] V. Nickich, T. Hegemann, M. Bartsch, G.F. Hanne, *Z. Phys. D, Atoms Mol., Clusters* **16,** 261 (1990).

[14] N. Andersen, J.W. Gallagher, I.V. Hertel, *Phys. Rep.* **165,** 1 (1988).

[15] T. Stacewicz, *SPIE Proc.* **1711-10,** 63 (1992).

[16] T. Stacewicz, *Z. Phys. D, Atoms Mol., Clusters* **27,** 149 (1993).

[17] T. Stacewicz, *Acta Phys. Pol. A* **84,** 259 (1993).

[18] V. Karaganov, I. Bray, P.J.O. Teubner, *Phys. Rev. A* **59,** 4407 (1999).

[19] A. Pietruczuk, P. Kruk, T. Stacewicz, *Radiat. Phys. Chem.*, accepted for publication.

[20] V. Nesmeyanov, *Vapour Pressure of Elements*, Academic Press, New York 1963.

[21] T. Stacewicz, N.A. Gorbunov, P. Kozłowski, *Appl. Phys. B* **66,** 461 (1998).

[22] N.A. Gorbunov, A. Grochola, P. Kruk, A. Pietruczuk, T. Stacewicz, *Plasma Sources Sci. Technol.* **11,** 492 (2002).

[23] T. Stacewicz, M. Kraińska-Miszczak, *Meas. Sci. Technol.* **8,** 1 (1997).

[24] N.A. Krall, A.W. Trivelpiece, *Principles of Plasma Physics*, McGraw-Hill, New York 1973, Ch. 6.9.2.

[25] R.H. Huddlestone, S.L. Leonard, *Plasma Diagnostic Techniques*, Academic, New York 1965.

[26] T. Stacewicz, W. Latek, *Phys. Scr.* **42,** 658 (1990).

[27] T. Holstein, *Phys. Rev.* **83,** 1159 (1951).

[28] A. Lindgard, S.E. Nielsen, *At. Data Nucl. Data Tables* **19,** 533 (1977).

[29] S.T. Chen, A.C. Gallagher, *Phys. Rev. A* **17,** 551 (1978).

[30] A. Zajonc, A. Gallagher, *Phys. Rev. A* **20,** 1393 (1979).

[31] L. Vušković, S. Trajmar, D.F. Register, *J. Phys. B, At. Mol. Phys.* **15,** 2517 (1982).

[32] B. Dubreil, C. Chaleard, *Phys. Rev. A* **29,** 958 (1984).

[33] C. Chaleard, B. Dobreuil, A. Catherinot, *Phys. Rev. A* **26,** 1431 (1982).